

Oil & Natural Gas Technology

DOE Award No.: DE-FE0010406
DUNS No.: 170230239

Quarterly Research Performance Progress Report (Period ending 6/30/2014)

CONTROLS ON METHANE EXPULSION DURING MELTING OF NATURAL GAS HYDRATE SYSTEMS: TOPIC AREA 2

Project Period (9/30/2013 to 6/30/2014)

Submitted by:
Peter B. Flemings



Signature

The University of Texas at Austin
101 East 27th Street, Suite 4.300
Austin, TX 78712-1500

e-mail: pflerings@jsg.utexas.edu

Phone number: 512-475-9520

Prepared for:
United States Department of Energy
National Energy Technology Laboratory

August 1, 2014



Office of Fossil Energy



1 ACCOMPLISHMENTS:

1.1 *What are the major goals of the project?*

The project goal is to predict, given characteristic climate-induced temperature change scenarios, the conditions under which gas will be expelled from existing accumulations of gas hydrate into the shallow ocean or directly to the atmosphere. When those conditions are met, the fraction of the gas accumulation that escapes and the rate of escape shall be quantified. The predictions shall be applicable in Arctic regions and in gas hydrate systems at the up dip limit of the stability zone on continental margins. The behavior shall be explored in response to two warming scenarios: longer term change due to sea level rise (e.g. 20 thousand years) and shorter term due to atmospheric warming by anthropogenic forcing (decadal time scale).

Milestone Description	Planned Completion	Actual Completion	Verification Method	Comments (progress toward achieving milestone, explanation of deviation from plan, etc.)
1.A 1-D simulation of gas hydrate dissociation in natural systems.	9/30/2013	9/30/2013	Report	We have completed this milestone and the results are documented in the continuation application.
1.B 1-D Simulation of gas hydrate dissociation in laboratory controlled conditions.	3/31/2014	11/1/2013	Report	We have completed this milestone and the results are documented in the continuation application.
1.C Model-based determination of conditions required for gas not to reach seafloor/atmosphere from dissociating hydrate accumulation.	3/31/2014	3/31/2014	Quarterly Report	We have completed this milestone and the results are documented in the continuation application.
1.D Determination of what hydrate reservoirs are at three-phase equilibrium.	12/31/2013	12/1/2013	Report	We have completed this milestone and the results are documented in the continuation application.
1.E Demonstrate ability to create and dissociate methane hydrate within sediment columns under conditions analogous to natural systems.	9/30/2013	10/15/2013	Report	We have completed this milestone and the results are documented in the continuation application.
2.A 1-D simulation of gas expulsion into hydrate stability zone.	9/29/2014		Report	Preliminary simulations produced
2.B Determination of conditions for which gas expulsion into hydrate-stability zone is self-limiting.	12/29/2014		Report	Preliminary simulations produced
2.C Demonstration of reaction transport experiment where gas invades hydrate stability zone and creates three phase stability.	9/30/2014		Quarterly Report	Currently developing/refining remote sensing technologies. Refining experimental design based on numerical simulation

2.D Demonstrate a 2D simulation of hydrate dissociation and gas expulsion.	3/31/2015		Report	
--	-----------	--	--------	--

1.2 What was accomplished under these goals?

1.21 Task 1: Project Management and Planning:

Projected Finish: 9/30/15

Actual Finish: In process

- 1) Organized and participated in web meeting presentation on project continuation.
- 2) Completed financial and status reports for sponsor.

1.22 Task 2: Conceptual and Numerical Model Development -1D

Projected Finish: 3/31/14

Actual Finish: 3/31/14

Summary:

Task 2 has been completed. We report on subtask (2.3.1) where we simulated the effect of warming on a deposit in a sub permafrost deposit below

1.22a Subtask 2.3 - 1D models of natural examples

Subtask 2.3.1 Hydrate accumulations below permafrost

A one-dimensional multiphase multicomponent fluid and heat flow and transport model is developed to investigate the permafrost and methane hydrate dynamics. This model is developed on basis of the numerical model of Liu and Flemings (2007). This model includes four phases (β), liquid (l), ice (i), free gas (v) and hydrate (h) phases, and three components (κ), water (w), methane (m) and salt (s). The liquid phase consists of water, methane and salt, the ice phase consists of only water, the vapor phase consists of only methane, and the hydrate phase consists of water and methane. We consider the pressure, capillary and density-driven fluid flow, advective and diffusive mass transport, and conductive and advective heat transport. The latent heat for ice and hydrate formation and dissociation is also taken into account. We use the model described in Moridis et al. (2008) to describe the phase boundary of methane hydrate and the model described in Sun and Mohanty (2006) to describe the phase boundary of ice. Ice is assumed to change the sediment properties in the same way as methane hydrate as described in Liu and Flemings (2007).

We apply this model to predict the response of permafrost and hydrate to future climate warming at Mallik site. Initially, the water pressure is hydrostatic with the fluid density of 1010 kg m^{-3} (Figure 1). The temperature at ground surface is set to be $-6 \text{ }^\circ\text{C}$ (Majorowicz et al., 2012), which increases linearly with a gradient of $8.3 \text{ }^\circ\text{C km}^{-1}$ to the depth of 600 m and $26 \text{ }^\circ\text{C km}^{-1}$ to the depth of 1500 m (Figure 1) (Henninges et al., 2002). We set the thermal conductivity of the grain to be $9.3 \text{ W m}^{-1} \text{ }^\circ\text{C}^{-1}$ in presence of ice and $3.0 \text{ W m}^{-1} \text{ }^\circ\text{C}^{-1}$ in absence of ice (Wright et al., 2005), so the initial temperature distribution is equilibrium. Permafrost distributes from the ground surface to the depth of 600 m (Figure 1). Salinity of the formation water in the shallow depths of the Beaufort-Mackenzie basin is largely terrestrial and can be as low as 0.1-0.5 wt.% (Dallimore and Collett, 1998). Therefore, we calculate the initial ice saturation

based on mass conservation of salt and salinity of 0.5 wt.% before ice formation (Figure 1). Below permafrost, we set the seawater salinity, 3 wt.%, as the initial salinity (Figure 1) (Taylor et al., 2005). The magnetic resonance-derived gas hydrate saturation at Mallik 5L-38 well is set as the initial hydrate distribution (Figure 1) (Dallimore and Collett, 2005). The temperature at ground surface is increased linearly from -6 to 0 °C in 300 years to represent the global warming effect of doubling CO_2 concentration in atmosphere (Majorowicz et al., 2012). We set the lower boundary at 1400 m depth, where the geothermal flux is fixed to be 56 mW m^{-2} , which equilibrate with the initial temperature distribution.

The increase of the ground surface temperature gradually propagates to deep depths, which cause the ice and hydrate stability zone shrink from both upward and downward (Figure 2a). Ice melts from both ground surface and its base (Figure 2b). The melting rate is greater at the permafrost base (Figure 2b). Permafrost totally disappeared at about 33 k.y.. The latent heat of ice melting attenuates the heat transport to deep depth and buffers hydrate melting. Hydrate starts to melt from its base at about 15 kyrs, when more than 100 m of ice has already disappeared (Figure 2b). The melting of hydrate provides methane to shallow depth and secondary hydrate deposits there (Figure 2b). Hydrate and ice melting decreases the local salinity, while secondary hydrate formation increases the local salinity to the three-phase equilibrium value and allows gas passage through the hydrate deposits (Figure 2b and 2c). With increasing time, the whole hydrate deposit moves upward. Methane gas starts to vent at ground surface at about 38 k.y. (Figure 3), after which the methane gas flux fluctuates with time (Figure 3). The entire hydrate deposits disappear at about 66 kyrs, and residual gas saturation remained in the subsurface (Figure 2b and Figure 3). If we decrease the initial ice saturation by 50%, the ice buffering effect is decreased and hydrate starts to melt at about 29 k.y., and the entire hydrate deposits disappears at about 57 k.y. (Figure 3). If we further decrease the ice saturation to zero at each depth, hydrate starts to melt at about 20 k.y., and the entire hydrate deposits disappears at about 46 kyrs (Figure 3). Based on this data, we find that about 4450 kg m^{-2} ice in the subsurface can delay the hydrate melting process by 9 kyrs. However, the total methane gas released at ground surface is fixed and determined by the initial total hydrate amount in the subsurface (Figure 4). The initial ice amount has negligible influence on the hydrate melting rate once hydrate starts to melt (Figure 4).

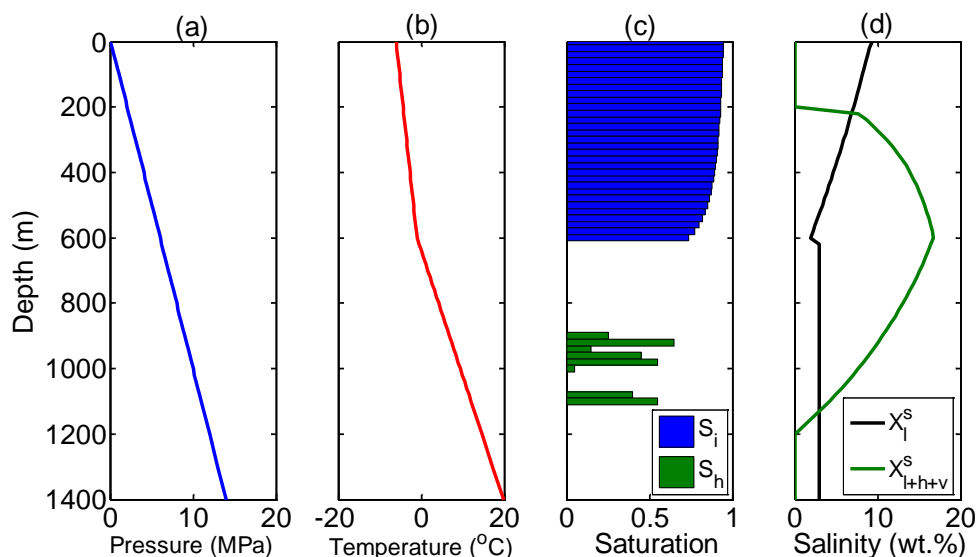
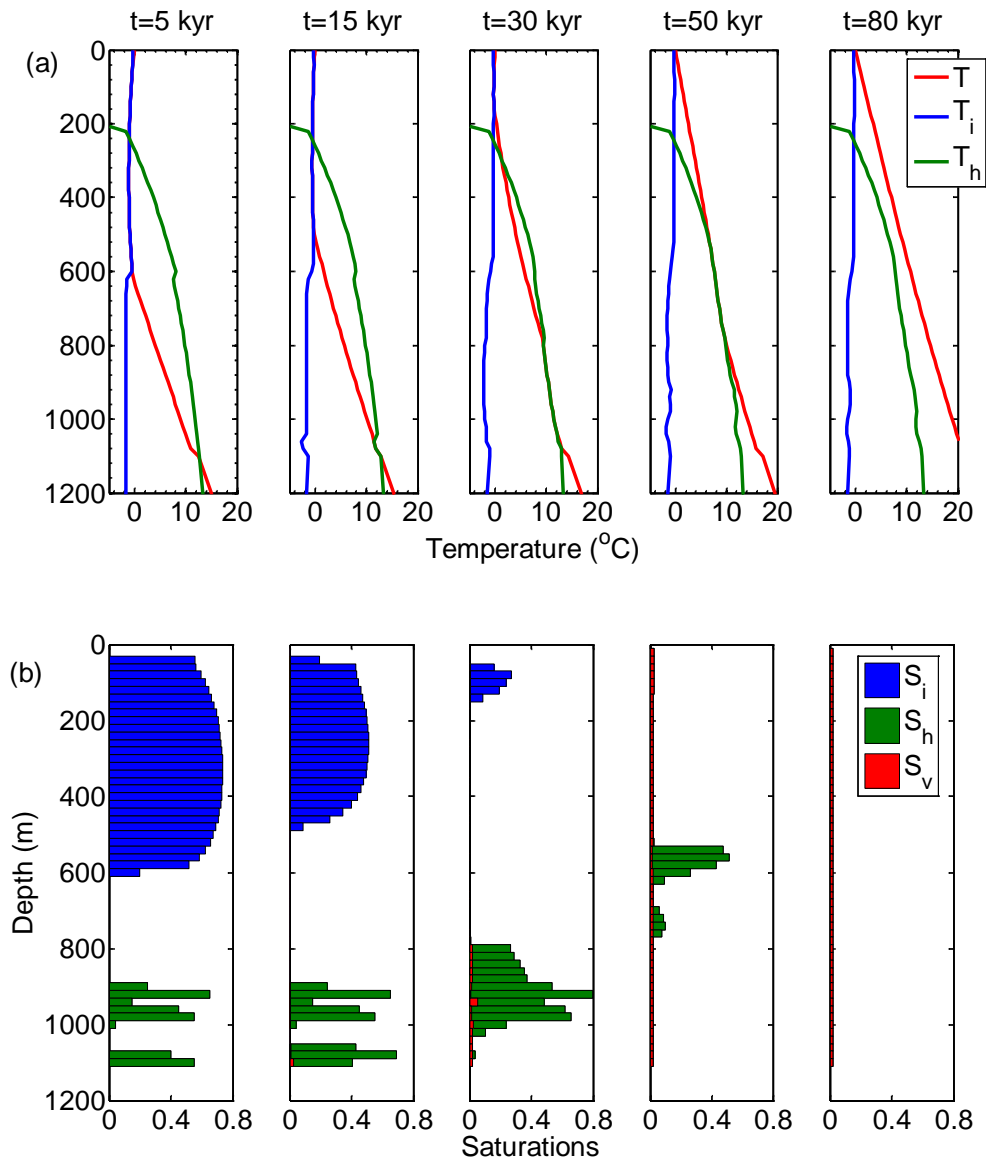


Figure 1: Initial (a) pressure, (b) temperature, (c) ice (S_i) and hydrate (S_h) saturation, (d) salinity (X_i^s) and three-phase (gas, water and hydrate phases) equilibrium salinity (X_{i+h+v}^s) distribution.



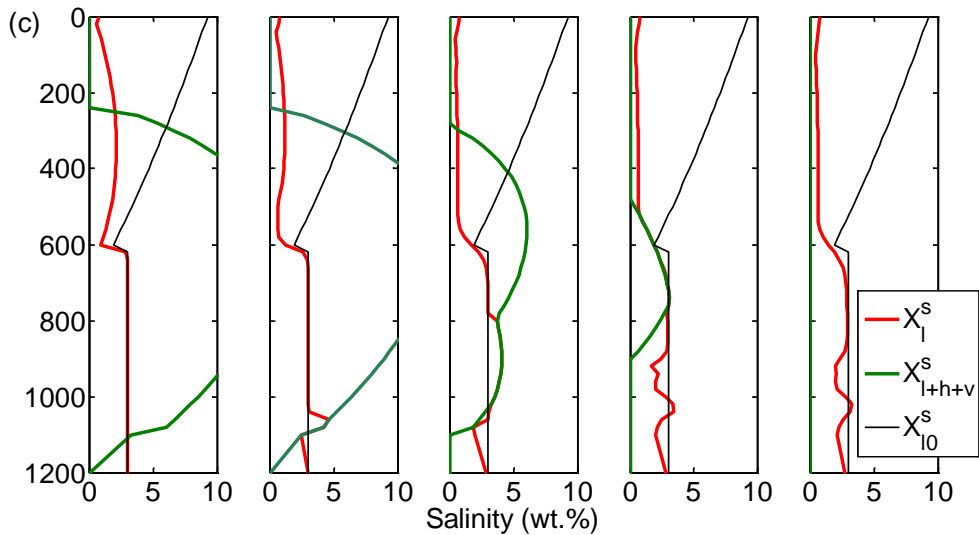


Figure 2: Evolution of (a) subsurface temperature (T), equilibrium temperature for ice and liquid (T_i), and three-phase equilibrium temperature for liquid, gas and hydrate (T_h), (b) ice (S_i), hydrate (S_h) and gas saturation (S_v), (c) salinity (X_i^s), three-phase equilibrium salinity for liquid, gas and hydrate (X_{l+h+v}^s) and initial salinity (X_{i0}^s) at 5, 15, 30, 50 and 80 kyr, respectively. In Figure 2(a), when blue line overlays red line, ice coexist with brine; when blue line is on the left of red line, ice is unstable. When green line overlays red line, hydrate, gas and brine coexist; when green line is on the right side of red line, hydrate is stable.

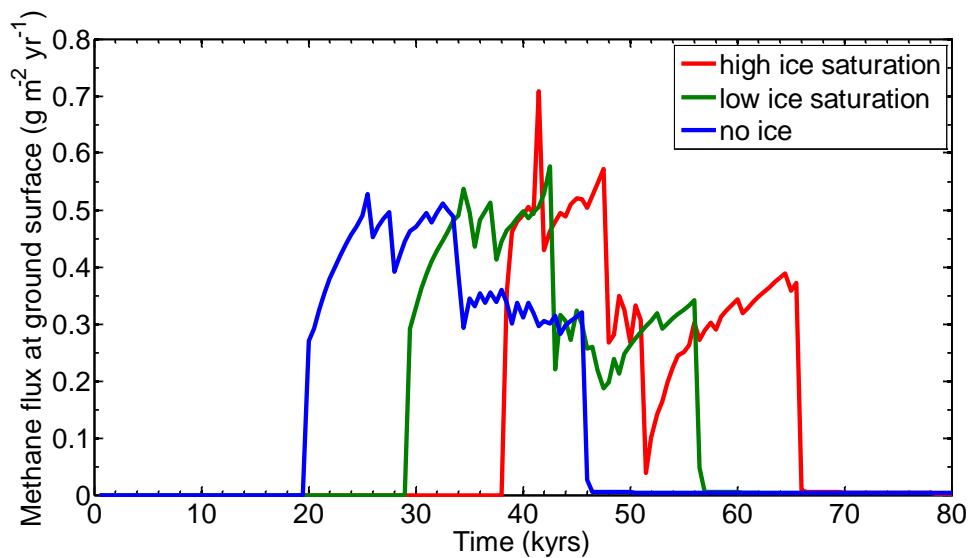


Figure 3: Evolution of methane gas flux at ground surface when the initial ice saturation is high, low and zero.

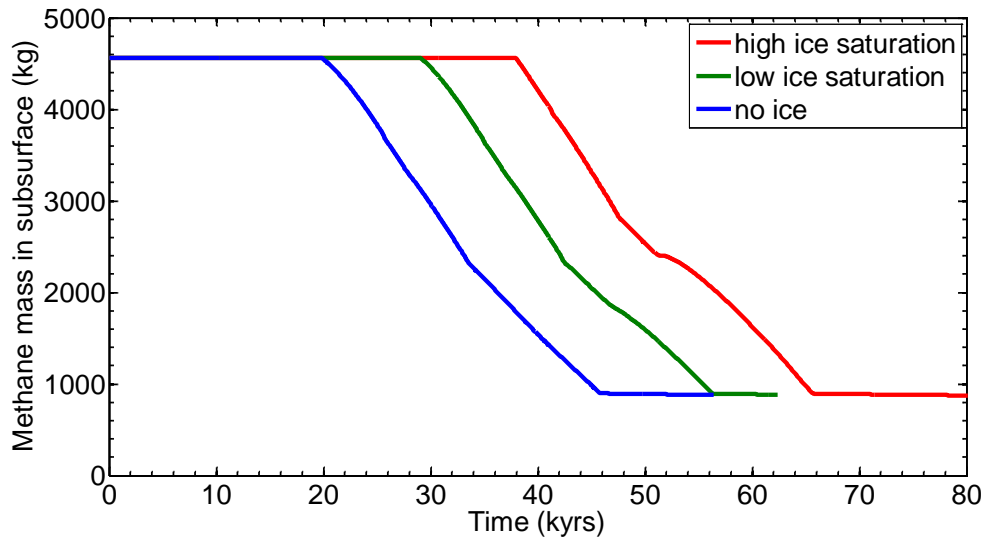


Figure 4: Evolution of total methane mass remained in subsurface when the initial ice saturation is high, low and zero.

Subtask 2.3.2 - 1D model application to deposits near up-dip limit of stability zone on continental margins

Subtask 2.3.2 has been completed and update given on a previous report.

1.23 Task 3: Categorize stability of known hydrate reservoirs

Projected Finish: 9/30/13

Actual Finish: 9/30/13

Milestone 1.D Determination of what hydrate reservoirs are at three-phase equilibrium.

Summary:

Task 3 has been completed and update given on a previous report.

1.24 Task 4: Laboratory Evaluation of Hydrate Dissociation

Projected Finish: 3/31/14

Actual Finish: 6/1/14

Summary

During this quarter, we have run a second experiment to simulate gas propagation in the hydrate stability zone. We report on these experiments below.

Subtask 4.1 - Freezing to 3 phase stability conditions, followed by melting from above

Milestone 1.E Demonstrate the ability to create and dissociate methane hydrate within sediment columns under conditions analogous to natural systems.

1.24a Subtask 4.3 - Freezing to L+H condition, warming from below

We previously described the geometry for our second experiment (Figure 5)

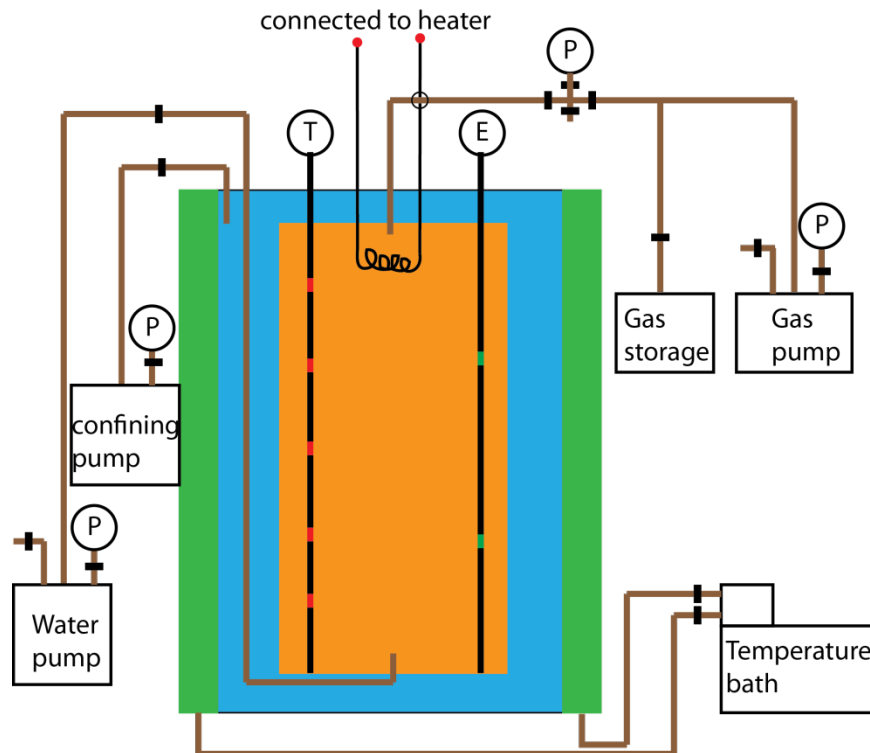


Figure 5: Schematic of the experimental setup. T means thermocouples. P means pressure transducers. E means electrodes measuring the bulk resistivity of the sample.

Initially, the sediment is saturated with brine of salinity 7 wt.%. The initial pressure in the column is set to be 6.89 MPa. During the experiment, we keep the temperature in the column to be 4 °C. We keep a constant gas pressure of 6.94 MPa at the top of the column, and pulling brine at 0.003 mL/min for 30 hours, 0 mL/min for 19.1 hours, 0.006 mL/min for 5.2 hours, and 0 mL/min for about 280 hours from the bottom of the column. During the experiment, we monitor the total brine and gas pump volume change (Figures 6 and 7) and the resistance change between the two electrodes (Figure 5 and 10). We also collect CT images to observe the density change in the column (Figure 8).

Total brine pump volume change is expected to reflect the total volume of brine pulled out from the sediment column. The measured total brine pump volume change starts with a value of 6 mL, and the rate of which is about 0.0056 mL/min in the first 30 hours (almost twice of the expected rate of 0.003 mL/min) (blue line with diamond markers in Figure 6). However, after 30 hours, the rate of total brine pump volume change matches the expected value described above. Therefore, there might be some operational error during the first 30 hours of the experiment, but it is corrected after that.

We conducted two simulations for this experiment using the 1D numerical model described in the last report. The first simulation is called hydrate formation, which exactly represents the condition in this experiment. The second simulation is called gas injection, where we increase the initial brine salinity to 12 wt.%, which is beyond methane hydrate stability condition. This simulation reflects gas replacing brine in the column. Brine volume leaving the column in hydrate formation simulation matches the expected result, while that in gas injection simulation is slightly lower than the expected one.

Total gas pump volume change is expected to reflect the volume of methane gas flowing into the sediment column. During the first 140 hours of the experiment, the measured total gas pump volume change is between the gas volume flowing into the column predicted in hydrate formation and gas injection simulations (Figure 7). After 140 hours, the measured value is greater than the predicted one in hydrate formation simulation (Figure 7). The predicted gas volume change in hydrate formation simulation reflects the maximum gas volume change if no leakage happens, and the predicted one in gas injection simulation reflects the minimum one. Therefore, there might be some hydrate formation, and there must be fluid leakage in the experiment.

CT images show that bulk density decreases at the top and along the side of the column during the early time of the experiment, and in the entire column during the late time (Figure 8a). Sequential change CT images show that the bulk density greatly decreases from 0 to 22 hours at the top and along the side of the column (Figure 8b), which can be explained as gas replacing brine during the first 22 hours there. The bulk density increases from 22 to 46 hours at the top of the column (Figure 8b), and hydrate could have formed there during this time period. More gas flows into the column, displaces brine and decreases the bulk density along the side. More hydrate could have formed in the center of the top column from 46 to 98 hours at the expense hydrate dissociation along the side of the column or brine migration out from there. With time goes on, there are some mild density decrease in the center of the lower part of the column although no more brine is being removed (Figure 8b). This could be caused by the capillary-driven brine flow toward the top of the column due to the decreased pore size there. This can also be explained as gas moving from the side to the center of the column.

In our hydrate formation simulation, hydrate forms immediately when methane gas reaches the brine in the column (Figure 9). However, in the experiment, more than 20 hours of induction time is required for hydrate nucleation (Figure 8). At 54.5 hours, hydrate reaction front is expected to reach the depth of 7 cm from the top of the column and stays there during the following time (Figure 9). However, hydrate reaction front seems only reach the depth of about 3 cm in the experiment (Figure 8). And we did not observe a gradually downward propagating hydrate reaction front with time as expected in the experiment. This could be caused by the difficulty of hydrate nucleation discussed in previous reports.

From 0 to 30 hours, gas injection and hydrate formation at the top of the column decreases the pore brine connectivity there, and the resistance increases with time (Figure 10). From 30 to about 200 hours, the resistance first sharply then gradually decreases with time (Figure 10), which is similar to the behavior in our first experiment and could be explained as pore-scale hydrate morphology change and column-scale hydrate reorganization. From 200 hours, the column-scale brine or gas migration could decrease the brine connectivity between the two electrodes (Figure 8), and sharply increase the resistance measured (Figure 10).

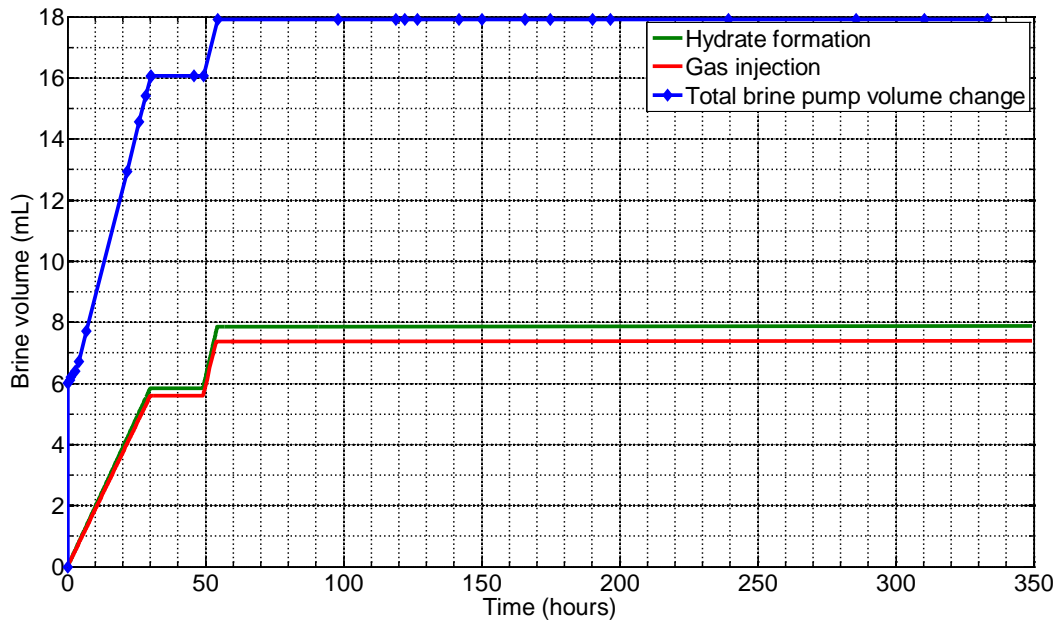


Figure 6: Evolution of measured brine pump volume change in the experiment and predicted brine volume decrease in the column in hydrate formation and gas injection simulations.

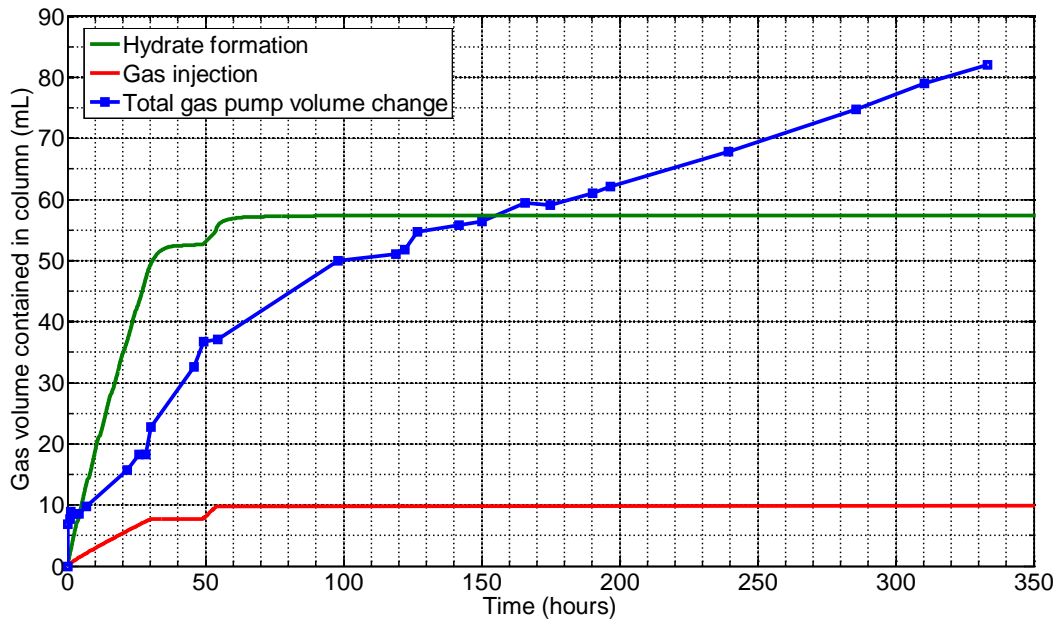


Figure 7: Evolution of measured gas pump volume change in the experiment and predicted gas volume injected into the column in hydrate formation and gas injection simulations.

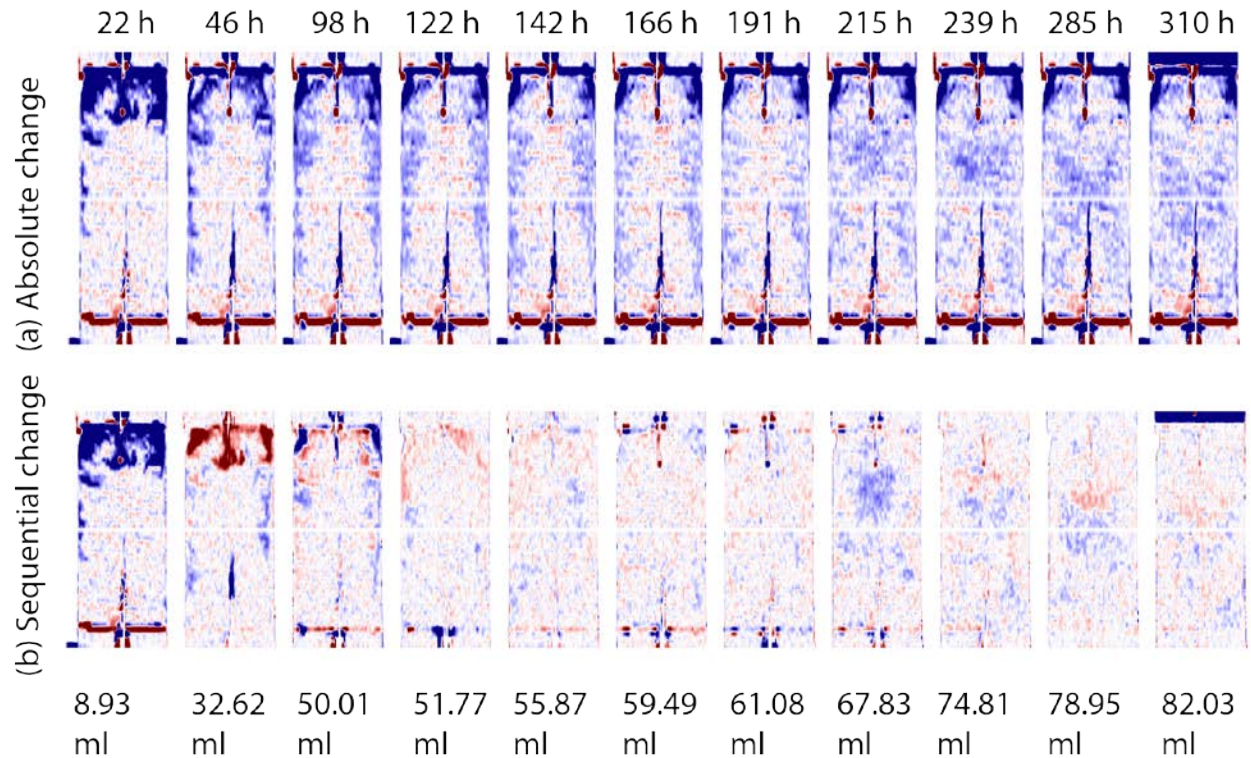


Figure 8: Evolution of (a) absolute bulk density change from the initial one and (b) bulk density change from the one measured at previous time when CT image is collected. Red color means density increase while blue color means density decrease. The darker the color, the greater the density change is. Numbers at the top of the figure represent the time when the data/CT images are collected. Numbers at the bottom of the figure represent the total gas pump volume decrease from initial value for each image.

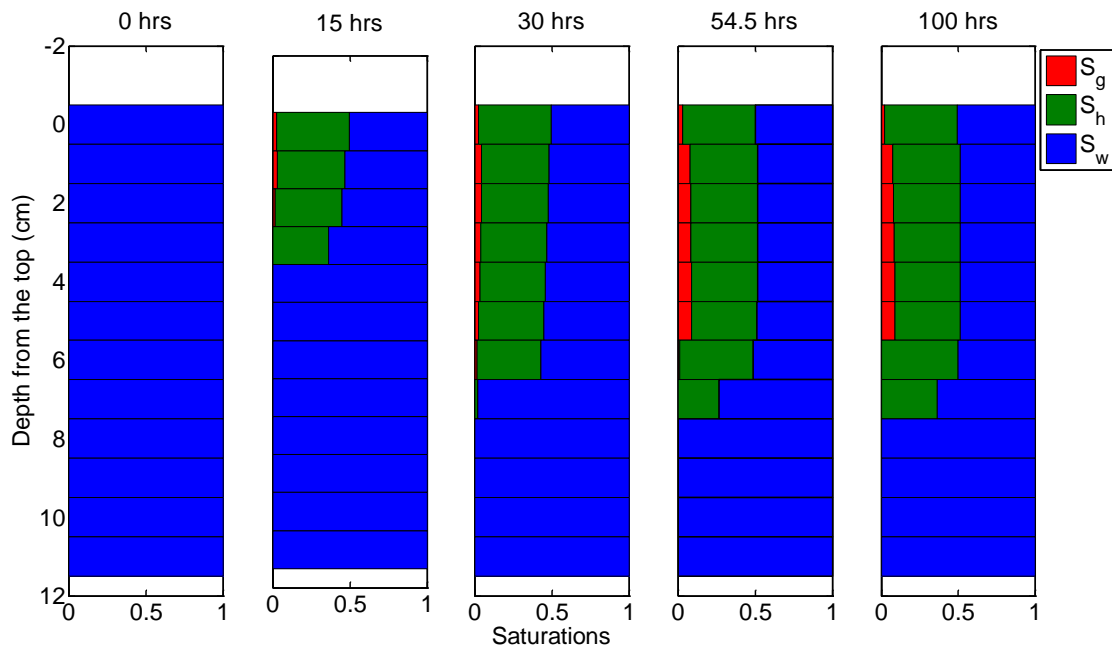


Figure 9: Predicted gas (S_g), hydrate (S_h) and water saturation (S_w) distribution at different time during the experiment.

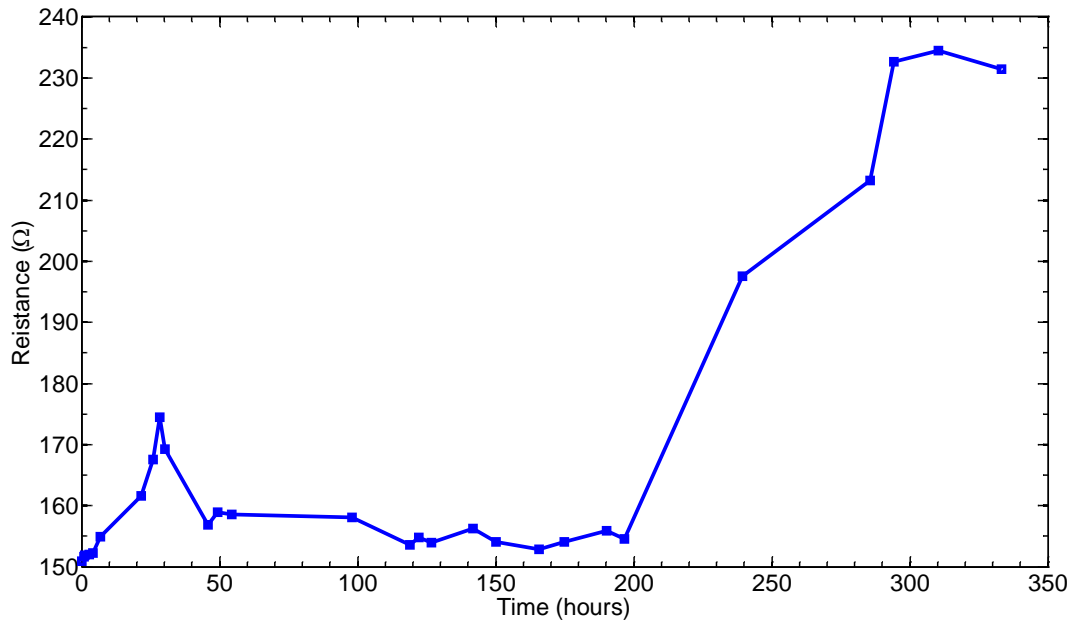


Figure 10: Evolution of resistance between the two electrodes during the experiment.

PHASE 2/BUDGET PERIOD 2

1.25 Task 5: Gas expulsion modeling

Projected Finish: 9/28/15

Actual Finish: in process

1.25a Subtask 5.1 - Develop 1D model of gas expulsion into water-saturated hydrate-stability zone

Projected Finish: 9/29/14

Actual Finish: in process

This model is fully developed and has been repeatedly presented in previous quarterly reports.

1.25b Subtask 5.2 - Apply 1D expulsion to laboratory experiments

Projected Finish: 3/30/15

Actual Finish: in process

The model has been developed (see Figure 9 above).

1.25c Subtask 5.3 - Apply 1D model to natural hydrate accumulations

Projected Finish: 9/28/15

Actual Finish: in process

The model is currently being applied to natural systems on the continental margins and in the permafrost zone in Alaska. See Figure 1-4 above.

1.26 Task 6: Gas expulsion experiments

Projected Finish: 9/28/15

Actual Finish: in process

1.26a Subtask 6.1 - Gas invasion into water-saturated hydrate saturated zone

Projected Finish: 12/29/14

Actual Finish: in process

Our first attempt at this is illustrated in Fig. 6-10 above. We have yet to be able to clearly propagate a gas invasion front into the water-saturated hydrate stability zone.

1.26b Subtask 6.2 - Gas invasion from melting hydrate into water saturated HSZ

Projected Finish: 9/28/15

Actual Finish: in process

We have not begun this task.

1.27 Task 7: 2D model

Projected Finish: 9/28/15

Actual Finish: in process

We have not begun this task.

1.27a Subtask 7.1 - Hydrate dissociation in 2D systems

Projected Finish: 9/29/14

Actual Finish: in process

We have not begun this task.

1.27b Subtask 7.2 - Gas expulsion in 2D systems

Projected Finish: 3/30/15

Actual Finish: in process

We have not begun this task.

1.27c Subtask 7.3 - Apply 2D, gas expulsion model to natural examples

Projected Finish: 9/28/15

Actual Finish: in process

We have not begun this task.

Subtask 7.3.1 Pleistocene to Holocene Sea level rise

Projected Finish: 9/28/15

Actual Finish: in process

We have not begun this task.

Subtask 7.3.2 - Recent warming

Projected Finish: 9/28/15

Actual Finish: in process

We have not begun this task.

1.3 What opportunities for training and professional development has the project provided?

There has been strong interaction between UT and LBNL over this past quarter. Our graduate students and our post-doctoral scientist are now fully working with both institutions. A particularly ripe interface is that our students and post-doc are working closely with experimental efforts at LBNL. There is continuous interaction between petroleum engineering and geosciences as we address this problem.

1.4 How have the results been disseminated to communities of interest?

Abstract and Paper Submissions

- Bhandari, A., Cronin, M., Polito, P., Flemings, P.B., Bryant, S., 2013, Mass Transport Properties in the Matrix of the Barnett Shale, Abstract submitted to be presented at *2013 Fall Meeting, AGU*, San Francisco, Calif., 9-13 Dec.
- Darnell, K., Flemings, P.B., Bryant, S., 2014, Simulations of seafloor methane venting from warming-induced hydrate destabilization, Abstract submitted to be presented at *8th International Conference on Gas Hydrates* Beijing, China, 28 July to 1 August 2014.
- Darnell, K., Flemings, P.B., 2013, Methane hydrate destabilization sensitivity to physical complexity and initial conditions in a numerical model, Abstract submitted to be presented at *2013 Fall Meeting, AGU*, San Francisco, Calif., 9-13 Dec.
- Kneafsey, T., Flemings, P.B., Bryant, S., You, K., Polito, P., 2013, Preliminary Experimental Examination Of Controls On Methane Expulsion During Melting Of Natural Gas Hydrate Systems, Abstract submitted to be presented at *2013 Fall Meeting, AGU*, San Francisco, Calif., 9-13 Dec.
- Meyer, D., Flemings, P.B., 2013, Thermodynamic state of hydrate-bearing sediments on continental margins around the world, Abstract submitted to be presented at *2013 Fall Meeting, AGU*, San Francisco, Calif., 9-13 Dec.
- Meyer, D., Flemings, P.B., 2014, Thermodynamic State of Hydrate-Bearing Sediments on Continental Margins Around the World, Abstract submitted to be presented at *2014 Offshore Technology Conference*, Houston, TX, 5-8 May.
- You, K., Flemings, P.B., Bryant, S., Kneafsey, T., Polito, P., 2014, Methane Hydrate Formation and Dissociation at Three-Phase Equilibrium at Constant Pressure, Abstract submitted to be presented at *8th International Conference on Gas Hydrates*, Beijing, China, 28 July to 1 August 2014.
- You, K., Flemings, P.B., Bryant, S., Kneafsey, T., Polito, P., 2014, Methane Hydrate Formation And Dissociation At Three-Phase Equilibrium At Constant Pressure, Abstract submitted to be presented at *Gordon Research Conference: Natural Gas Hydrate Systems*, Galveston, TX, 23-28 March.

- You, K., Flemings, P.B., Bryant, S., Kneafsey, T., Polito, P., 2014, Salinity-buffered methane hydrate formation and dissociation in gas-rich systems, *Journal of Geophysical Research: Solid Earth*, in review.

1.5 What do you plan to do during the next reporting period to accomplish the goals?

1.51 Task 5.00: Gas expulsion modeling

Subtask 5.10: Develop 1D model of gas exp. into water-sat. hydrate-stability zone

Subtask 5.20: Apply 1D expulsion to laboratory experiments

We have developed the model for laboratory experiments and reported on that above. Our experiment, however, has not produced a stable advancing gas front. We will focus on developing a stable advancing gas front in the coming quarter in our experimental apparatus.

Subtask 5.30: Apply 1D model to natural hydrate accumulations

We have applied our 1D model to arctic systems and we will complete our write up on these systems.

1.52 Task 6.00: Gas expulsion experiments

Subtask 6.10: Gas invasion into water-saturated hydrate saturated zone

Subtask 6.20: Gas invasion from melting hydrate into water saturated HSZ

We will continue to pursue our experiments at LBNL. Our biggest challenge is to successfully produce a hydrate saturation solidification front.

1.53 Task 7.00: 2D model

Subtask 7.10: Hydrate dissociation in 2D systems

We will begin work on this task in the coming quarter.

Subtask 7.20: Gas expulsion in 2D systems

We will begin work on this task in the coming quarter.

Subtask 7.30: Apply 2D, gas expulsion model to natural examples

Subtask 7.31: Pleistocene to Holocene Sea level rise

Subtask 7.32: Recent warming

2 PRODUCTS:

2.1 What has the project produced?

We have now produced a one dimensional, coupled; hydrate formation code that simulates the thermochemical response of a hydrate system to perturbation. We have demonstrated three-phase stability through experimental analysis and we have modeled the behavior. We have also characterized the in-situ thermodynamic state of a number of hydrate locations around the world and shown that in at least two locations, local thermodynamic conditions are altered by high salinity.

3 PARTICIPANTS & OTHER COLLABORATING ORGANIZATIONS:

3.1 What individuals have worked on the project?

Provide the following information for: (1) principal investigator(s)/project director(s) (PIs/PDs); and (2) each person who has worked at least one person month per year on the project during the reporting period, regardless of the source of compensation (a person month equals approximately 160 hours of effort).

Name	Peter Flemings	Steve Bryant	Tim Kneafsey	Dylan Meyer	Ebrahim Roasromani
Project Role	Principal Investigator	Co-Principal Investigator	Co-Principal Investigator	Graduate Student	Graduate Student
Nearest person month worked	.25	.25	1.25	1	1
Contribution	Advised graduate student Meyer, managed project, and recruited students. Worked with technicians for thermistor development.	Advised graduate student Meyer on analysis of models of pore space alteration due to hydrate growth and its effect on saturation exponent.	Set up experiment, ran tests, and analyzed data.	Performed analysis of thermodynamic state of 4 locations.	Performed analysis of data.
Funding Support	The University of Texas	The University of Texas	Lawrence Berkeley National Lab	JSG Fellowship	The University of Texas
Collaborated with individual in foreign country	No	No	No	No	No

Name	Peter Polito	Kris Darnell	Kehua You	Tessa Green	
Project Role	Laboratory Manager	Graduate Student	Post Doc	Project Coordinator	
Nearest person month worked	1.5	1	3	1	
Contribution	Participated in conference calls on experimental design. Ran experimental tests.	Performed literature review and theoretical calculation to prepare for laboratory experiments	Performed literature review and theoretical calculation to prepare for laboratory experiments	Coordinate meeting logistics, archive documents, and manage financials.	
Funding Support	The University of Texas	The University of Texas	The University of Texas	The University of Texas	
Collaborated with individual in foreign	No	No	No	No	

country					
---------	--	--	--	--	--

3.2 What other organizations have been involved as partners?

Organization Name: Lawrence Berkeley National Lab

Location of Organization: Berkeley, CA

Partner's contribution to the project (identify one or more)

- In-kind support: partner makes lab space and equipment available for experiments. (e.g., partner makes software, computers, equipment, etc., available to project staff);
- Facilities: Experiments are performed in partner's lab space using equipment largely supplied by the partner (e.g., project staff use the partner's facilities for project activities);
- Collaborative research: Partner collaborates with the project staff. (e.g., partner's staff work with project staff on the project); and

3.3 Have other collaborators or contacts been involved?

No

4 IMPACT:

4.1 What is the impact on the development of the principal discipline(s) of the project?

Geological models of gas transport and hydrate melting and solidification have suggested that free gas cannot migrate through the hydrate stability zone during melting. In contrast, we suggest that free gas can migrate through the hydrate stability zone by altering the conditions of hydrate stability to a state of three-phase equilibrium through the elevation of salinity and possibly temperature. This results in fundamentally different macro-scale behavior during melting and may result in greater gas venting than has been previously demonstrated. If this hypothesis is correct, it may engender a new generation of field and laboratory investigations to document this behavior in both the field of geosciences and petroleum engineering. Second, the project links theoretical development with laboratory modeling because the concepts can be applied at the laboratory scale as well as the field scale. The laboratory experiments to be conducted will enable validation of the mechanisms incorporated in the models. These laboratory experiments will play a key role in demonstrating the processes.

4.2 What is the impact on other disciplines?

A likely outcome of our work is a more quantitative prediction of the magnitude of methane flux from the earth to the atmosphere over human (decadal) timescales and geological timescales (10,000 years). These will serve as boundary conditions for atmospheric climate models. In turn, these results may guide policy decisions.

4.3 What is the impact on the development of human resources?

We are working at the interface of geosciences and engineering. We are coupling theory and laboratory experiments to address macro-scale geologic problems. This is training a new generation of geoscientists and engineers to think with a systems-based approach that links observation with theory.

The results are being applied in the classroom and the support is training several graduate students.

4.4 *What is the impact on physical, institutional, and information resources that form infrastructure?*

The project is strengthening the experimental efforts and capability at UT as it is our job to develop sensor equipment. The project is strengthening development at LBNL where primary experimental work is occurring.

4.5 *What is the impact on technology transfer?*

We are presenting our research to approximately 100 industry members at our GeoFluids consortium and we will be presenting at a range of national and international meetings. We will also present our results at the upcoming OTC conference in Spring 2014.

4.6 *What is the impact on society beyond science and technology?*

A likely outcome of our work is a more quantitative prediction of the magnitude of methane flux from the earth to the atmosphere over human (decadal) timescales and geological timescales (10,000 years). These will serve as boundary conditions for atmospheric climate models. In turn, these results may guide policy decisions.

4.7 *What dollar amount of the award's budget is being spent in foreign country(ies)?*

Zero percent of the award's budget is being spent in foreign countries.

5 CHANGES/PROBLEMS:

5.1 *Changes in approach and reasons for change*

There are no changes in approach to report for this reporting period.

5.2 *Actual or anticipated problems or delays and actions or plans to resolve them*

Our biggest challenge is in the experimental realm. It has been more challenging than envisioned to simulate the solidification of hydrate with an advancing gas front. LBNL is also nearly spent out of resources. We are evaluating next steps.

5.3 *Changes that have a significant impact on expenditures*

No changes in approach to report for this reporting period.

5.4 *Significant changes in use or care of human subjects, vertebrate animals, and/or Biohazards*

Nothing to report

5.5 *Change of primary performance site location from that originally proposed*

Nothing to report

6 BUDGETARY INFORMATION:

	Budget Period 1											
	Q1			Q2			Q3			Q4		
	10/1/12 - 2/15/13	Cumulative Total	2/16/13-6/30/2013	Cumulative Total	7/1/2013-11/15/2013	Cumulative Total	11/16/2013-3/31/2014	Cumulative Total				
Baseline Reporting (10/1/12 - 6/30/14)												
Baseline Cost Plan												
Federal Share	\$ 136,111.50	\$ 136,111.50	\$ 175,000.50	\$ 311,112.00	\$ 175,000.50	\$ 486,112.50	\$ 175,000.50	\$ 661,113.00				
Non-Federal Share	\$ 43,568.75	\$ 43,568.75	\$ 43,568.75	\$ 87,137.50	\$ 43,568.75	\$ 130,706.25	\$ 43,568.75	\$ 174,275.00				
Total Planned	\$ 179,680.25	\$ 179,680.25	\$ 218,569.25	\$ 398,249.50	\$ 218,569.25	\$ 616,818.75	\$ 218,569.25	\$ 835,388.00				
Actual Incurred Cost												
Federal Share	\$ 45,506.00	\$ 45,506.00	\$ 67,607.00	\$ 113,113.00	\$ 258,059.00	\$ 371,172.00	\$ 137,004.00	\$ 508,176.00				
Non-Federal Share	\$ -	\$ -	\$ 81,202.43	\$ 81,202.43	\$ 26,527.09	\$ 107,729.52	\$ 10,775.81	\$ 118,505.33				
Total Incurred Cost	\$ 45,506.00	\$ 45,506.00	\$ 148,809.43	\$ 194,315.43	\$ 284,586.09	\$ 478,901.52	\$ 147,779.81	\$ 626,681.33				
Variance												
Federal Share	\$ (90,605.50)	\$ (90,605.50)	\$ (107,393.50)	\$ (197,999.00)	\$ 83,058.50	\$ (114,940.50)	\$ (37,996.50)	\$ (152,937.00)				
Non-Federal Share	\$ (43,568.75)	\$ (43,568.75)	\$ 37,633.68	\$ (5,935.07)	\$ (17,041.66)	\$ (22,976.73)	\$ (32,792.94)	\$ (55,769.67)				
Total Variances	\$ (134,174.25)	\$ (134,174.25)	\$ (69,759.82)	\$ (203,934.07)	\$ 66,016.84	\$ (137,917.23)	\$ (70,789.44)	\$ (208,706.67)				
	Budget Period 2											
	Q1			Q2			Q3			Q4		
	4/1/2014-8/15/2014			8/16/2014-12/31/2014			1/1/2015-5/15/2015			5/16/2015-9/30/2015		
Baseline Cost Plan												
Federal Share	\$ 127,422.00	\$ 661,113.00	\$ 127,422.00	\$ 788,535.00	\$ 127,422.00	\$ 915,957.00	\$ 127,422.00	\$ 1,043,379.00				
Non-Federal Share	\$ 34,048.50	\$ 174,275.00	\$ 34,048.50	\$ 208,323.50	\$ 34,048.50	\$ 242,372.00	\$ 34,048.50	\$ 276,420.50				
Total Planned	\$ 161,470.50	\$ 835,388.00	\$ 161,470.50	\$ 996,858.50	\$ 161,470.50	\$ 1,158,329.00	\$ 161,470.50	\$ 1,319,799.50				
Actual Incurred Cost												
Federal Share	\$ 119,439.00	\$ 508,176.00	\$ -	\$ 508,176.00	\$ -	\$ 508,176.00	\$ -	\$ 508,176.00				
Non-Federal Share	\$ 10,000.00	\$ 118,505.33	\$ -	\$ 118,505.33	\$ -	\$ 118,505.33	\$ -	\$ 118,505.33				
Total Incurred Cost	\$ 129,439.00	\$ 626,681.33	\$ -	\$ 626,681.33	\$ -	\$ 626,681.33	\$ -	\$ 626,681.33				
Variance												
Federal Share	\$ (7,983.00)	\$ (152,937.00)	\$ (127,422.00)	\$ (280,359.00)	\$ (127,422.00)	\$ (407,781.00)	\$ (127,422.00)	\$ (535,203.00)				
Non-Federal Share	\$ (24,048.50)	\$ (55,769.67)	\$ (34,048.50)	\$ (89,818.17)	\$ (34,048.50)	\$ (123,866.67)	\$ (34,048.50)	\$ (157,915.17)				
Total Variances	\$ (32,031.50)	\$ (208,706.67)	\$ (161,470.50)	\$ (370,177.17)	\$ (161,470.50)	\$ (531,647.67)	\$ (161,470.50)	\$ (693,118.17)				

7 Nomenclatures

G	Free gas phase
H	Hydrate phase
L	Liquid phase
u	Pore pressure (MPa)
ρ_{sw}	Seawater Density (g/cm^3)
ρ_{pw}	Pore water density (g/cm^3)
ρ_f	Fluid density (g/cm^3)
ρ_b	Bulk density (g/cm^3)
ρ_m	Grain density (g/cm^3)
Z_{wd}	Water depth (m)
ΔZ	Depth within the GHSZ (m)
Z	GHSZ thickness (m)
g	Gravitational acceleration (m/s^2)
T_f	Formation temperature ($^{\circ}\text{C}$)
T_b	Seafloor temperature ($^{\circ}\text{C}$)
G_g	Geothermal gradient ($^{\circ}\text{C/km}$)
S_h	Hydrate saturation (dimensionless)
S_w	Water saturation (dimensionless)
$C_{in-situ}$	In-situ salinity (dimensionless)
C_0	Core-derived salinity (dimensionless)
C	Salinity (dimensionless)
N	Saturation exponent (dimensionless)
a	Tortuosity coefficient (dimensionless)
m	Cementation exponent (dimensionless)
n	Porosity (dimensionless)
ρ_w	Fluid resistivity (Ωm)
ρ_t	Formation resistivity (Ωm)
F	Formation factor (dimensionless)

Analytical model

M_m	molar weight of methane (kg mol^{-1})
M_w	molar weight of water (kg mol^{-1})
M_h	molar weight of hydrate (kg mol^{-1})
$m_{g,f}^m$	methane mass in the final gas phase (kg)
$m_{h,f}^m$	methane mass in the final hydrate phase (kg)
$m_{w,f}^m$	methane mass in the final water phase (kg)
$m_{g,i}^m$	methane mass in the initial gas phase (kg)
$m_{w,i}^m$	methane mass in the initial water phase (kg)
N	stoichiometric hydration number (dimensionless)
P_f	final pressure (Pa)
P_i	initial pressure (Pa)
T_f	final temperature (K)
T_i	initial temperature (K)
$S_{g,i}$	initial gas saturation (dimensionless)

$S_{g,f}$	final gas saturation (dimensionless)
$S_{h,f}$	maximum hydrate saturation (dimensionless)
$S_{w,i}$	initial water saturation (dimensionless)
$S_{w,f}$	final water saturation (dimensionless)
V_{tot}	total volume of the sediment (m^3)
$X_{w,f}^m$	final solubility of methane in water (wt.%)
$X_{w,i}^m$	initial solubility of methane in water (wt.%)
$X_{w,i}^s$	initial mass fraction of salt in brine (wt.%)
$X_{w,f}^s$	final mass fraction of salt in brine (wt.%)
$\rho_{w,f}$	initial brine density ($kg\ m^{-3}$)
$\rho_{w,i}$	final brine density ($kg\ m^{-3}$)
$\rho_{g,i}$	initial gas density ($kg\ m^{-3}$)
$\rho_{g,f}$	final gas density ($kg\ m^{-3}$)
ρ_h	methane hydrate density ($kg\ m^{-3}$)
ϕ	porosity of the sediment (dimensionless)
Δm	mass of methane gas consumed during hydrate formation (kg)

Numerical model

β	phase
e	energy component
g	gas phase
h	hydrate phase
κ	component
l	liquid phase
m	methane component
s	salt component
v	vapor phase
w	water component
C_R	heat capacity of the solid grain ($J\ kg^{-1}\ ^\circ C^{-1}$)
D_{T0}^{κ}	molecular diffusion coefficient of component κ in free water ($m^2\ s^{-1}$)
ϕ	porosity of the sediment (dimensionless)
ϕ_0	porosity in the absence of hydrate (dimensionless)
g	acceleration due to gravity ($m\ s^{-2}$)
h_{β}	specific enthalpy of phase β ($J\ kg^{-1}$)
k	intrinsic permeability (m^2)
k_0	permeability in the absence of hydrate (m^2)
$k_{r\beta}$	relative permeability of phase β (dimensionless)
λ	overall thermal conductivity of porous media ($W\ m^{-1}\ ^\circ C^{-1}$)
λ_{β}	thermal conductivity of phase β ($W\ m^{-1}\ ^\circ C^{-1}$)
λ_R	thermal conductivity of grain ($W\ m^{-1}\ ^\circ C^{-1}$)
μ_{β}	viscosity of phase β (Pa s)
P_c	capillary pressure (Pa)
P_{c0}	capillary pressure in the absence of hydrate (Pa)

P_{β}	β phase pressure (Pa)
q^e	generation rate of energy ($\text{J m}^{-3} \text{s}^{-1}$)
q^{κ}	generation rate of component κ ($\text{kg m}^{-3} \text{s}^{-1}$)
ρ_{β}	density of phase β (kg m^{-3})
S_{β}	saturation of phase β (dimensionless)
T	temperature ($^{\circ}\text{C}$)
t	time (s)
u_{β}	specific internal energy of phase β (J kg^{-1})
X_{β}^{κ}	mass fraction of component κ in phase β (dimensionless)

8 References

- Dallimore, S., and Collett, T., Gas Hydrates Associated With Deep Permafrost in the Mackenzie Delta, N.W.T., Canada: Regional Overview, *in* Proceedings PERMAFROST - Seventh International Conference (Proceedings), Yellowknife, Canada, 1998, Volume Collection Nordicana No 55.
- , 2005, Scientific results from the Mallik 2002 gas hydrate production research well program, Mackenzie delta, Northwest Territories, Geological Survey of Canada, Volume Bulletin 601.
- Henniges, J., Schrötter, J., Erbas, K., and Huenges, E., Temperature profiles during a gas hydrate production test, Gas Hydrates in the Geosystem, *in* Proceedings Status Seminar (Kiel 2002), Kiel, Germany, 2002.
- Liu, X., and Flemings, P. B., 2007, Dynamic multiphase flow model of hydrate formation in marine sediments: *Journal of Geophysical Research*, v. 112, no. B3.
- Majorowicz, J., Osadetz, K., and Safanda, J., 2012, Gas Hydrate Formation and Dissipation Histories in the Northern Margin of Canada: Beaufort-Mackenzie and the Sverdrup Basins: *Journal of Geological Research*, v. 2012.
- Moridis, G., 2008, TOUGH+Hydrate v1.0 User's Manual: A Code for the Simulation of System Behavior in Hydrate-Bearing Geologic Media.
- Sun, X., and Mohanty, K. K., 2006, Kinetic simulation of methane hydrate formation and dissociation in porous media: *Chemical Engineering Science*, v. 61, no. 11, p. 3476-3495.
- Taylor, A. E., Dallimore, S. R., Hyndman, R. D., and Wright, F., 2005, Comparing the sensitivity of terrestrial and marine gas hydrates to climate warming at the end of the last ice age.: *Geological Survey of Canada Bulletin*.
- Wright, J. F., Dallimore, S. R., Nixon, F. M., and Duchesne, C., 2005, In situ stability of gas hydrate in reservoir sediments of the JAPEx/JNOC/GSC et al. Mallik 5L-38 gas hydrate production well, *in* Dallimore, S. R., and Collett, T. S., ed., Scientific Results from the Mallik 2002 Gas Hydrate Production Research Well Program, Mackenzie Delta, Northwest Territories, Canada, Volume Bulletin 585, Geological Survey of Canada, p. 11.

National Energy Technology Laboratory

626 Cochrans Mill Road
P.O. Box 10940
Pittsburgh, PA 15236-0940

3610 Collins Ferry Road
P.O. Box 880
Morgantown, WV 26507-0880

13131 Dairy Ashford Road, Suite 225
Sugar Land, TX 77478

1450 Queen Avenue SW
Albany, OR 97321-2198

Arctic Energy Office
420 L Street, Suite 305
Anchorage, AK 99501

Visit the NETL website at:
www.netl.doe.gov

Customer Service Line:
1-800-553-7681

